Open Forum Infectious Diseases

MAJOR ARTICLE

Transcriptomic Predictors of Paradoxical Cryptococcosis-Associated Immune Reconstitution Inflammatory Syndrome

Irina Vlasova-St. Louis,[1,a] Christina C. Chang,[2,a] Samar Shahid,[1] Martyn A. French,[3] and Paul R. Bohjanen[1]

[1]Department of Medicine, Division of Infectious Diseases and International Medicine, Program in Infection and Immunity, University of Minnesota, Minneapolis; [2]Department of Infectious Diseases, Alfred Hospital, Melbourne and Monash University, Australia; [3]UWA Medical School and School of Biomedical Sciences, University of Western Australia, Perth, Australia

Background. Paradoxical cryptococcosis-associated immune reconstitution inflammatory syndrome (C-IRIS) affects ~25% of human immunodeficiency virus (HIV)-infected patients with cryptococcal meningitis (CM) after they commence antiretroviral therapy (ART) resulting in significant morbidity and mortality. Genomic studies in cryptococcal meningitis and C-IRIS are rarely performed.

Methods. We assessed whole blood transcriptomic profiles in 54 HIV-infected subjects with CM who developed C-IRIS (27) and compared the results with control subjects (27) who did not experience neurological deterioration over 24 weeks after ART initiation. Samples were analyzed by whole genome microarrays.

Results. The predictor screening algorithms identified the low expression of the components of interferon-driven antiviral defense pathways, such as interferon-inducible genes, and higher expression of transcripts that encode granulocyte-dependent proinflammatory response molecules as predictive biomarkers of subsequent C-IRIS. Subjects who developed early C-IRIS (occurred within 12 weeks of ART initiation) were characterized by upregulation of biomarker transcripts involved in innate immunity such as the inflammasome pathway, whereas those with late C-IRIS events (after 12 weeks of ART) were characterized by abnormal upregulation of transcripts expressed in T, B, and natural killer cells, such as IFNG, IL27, KLRB1, and others. The AIM2, BEX1, and C1QB were identified as novel biomarkers for both early and late C-IRIS events.

Conclusions. An inability to mount effective interferon-driven antiviral immune response, accompanied by a systemic granulocyte proinflammatory signature, prior to ART initiation, predisposes patients to the development of C-IRIS. Although early and late C-IRIS have seemingly similar clinical manifestations, they have different molecular phenotypes (as categorized by bioinformatics analysis) and are driven by contrasting inflammatory signaling cascades.

Keywords: cryptococcosis-associated immune reconstitution inflammatory syndrome (C-IRIS); AIDS/HIV; antiretroviral therapy; transcriptomic biomarkers.

Cryptococcal meningitis (CM) is responsible for 60% of meningitis-associated hospitalizations and deaths in persons with human immunodeficiency virus (HIV) in resource-limited settings [1, 2]. Moreover, ~25% of patients with CM who begin antifungal treatment and antiretroviral therapy (ART) experience neurological deterioration characterized by headaches, seizures, or confusion caused by paradoxical cryptococcosis-associated immune reconstitution inflammatory syndrome (C-IRIS) [3–5]. The risk factors associated with C-IRIS include an advanced state of immunosuppression ($CD4^+$ T-cell count less than 100 cells/μL) and high cryptococcal fungal burden at ART initiation [5, 6]. The clinical manifestations of C-IRIS usually begin within the first 4 weeks of ART initiation; however, late presentation beyond 12 weeks has also been reported [4, 7].

The pathogenesis of C-IRIS is still poorly understood. In the setting of immune reconstitution after initiation of effective ART, an exaggerated and dysregulated immune response toward cryptococcal antigens is hypothesized to drive the development of C-IRIS [8, 9]. Cryptococcosis-associated immune reconstitution inflammatory syndrome is associated with activation of multiple immune and inflammatory pathways, but few biomarkers have been reported to define C-IRIS [5, 10, 11]. There are no laboratory tests available in routine clinical practice to confirm C-IRIS, which makes diagnosis and treatment difficult. Thus, identifying a comprehensive transcriptomic signature of C-IRIS is an important step to understanding the pathogenesis of C-IRIS and to identify diagnostic and prognostic biomarkers.

In this study, we performed genome-wide transcriptomic analyses using microarrays to characterize ART-induced changes in gene expression in peripheral blood of HIV-infected

Received 19 March 2018; editorial decision 25 June 2018; accepted 26 June 2018.

[a]I. V.-S. and C. C. C. contributed equally to this work.

Correspondence: I. Vlasova-St. Louis, MD, PhD, Department of Medicine, Division of Infectious Diseases and International Medicine, Program in Infection and Immunity, University of Minnesota, Mayo Memorial Building Rm820, 420 Delaware St SE, Minneapolis, MN 55455 (irinastl@umn.edu).

Open Forum Infectious Diseases®

DOI: 10.1093/ofid/ofy157

individuals with CM who did or did not developed C-IRIS, to understand the immune dysregulation that causes C-IRIS and identify novel diagnostic and prognostic molecular biomarkers for C-IRIS.

METHODS

Study Setting and Sample Collection

This study used deidentified pre-existing samples obtained from the C-IRIS study performed in Durban, South Africa, which followed 130 HIV-infected subjects with confirmed CM for 24 weeks and determined which subjects developed C-IRIS and which did not [5]. Recruitment, follow-up of patients, and the criteria for C-IRIS diagnosis have previously been published (see Figure 1) [5]. Ethics approval for the parent study was obtained from University of KwaZulu-Natal (BF053/09, Monash University (2009001224, 2016-1197), University of Western Australia (RA/4/1/2541), and University of Minnesota (1007E86393).

For the current study, whole blood (2.5 mL) was collected into PAXgene tubes (QIAGEN Inc.) from 27 subjects who developed C-IRIS in the 6 months after ART commencement and from 27 $CD4^+$ T cell count-matched control subjects who did not develop neurological deterioration. Whole blood samples were collected at the time of ART initiation (W00), at weeks 4 and 12 (W4, W12) after ART commencement and at time of C-IRIS event (Figure 1). We categorized "early C-IRIS" events (21 samples) as those occurring within 12 weeks of ART and those occurring after 12 weeks as "late C-IRIS" (6 samples).

Ribonucleic Acid Extraction and Microarray Analyses

Total ribonucleic acid (RNA) was extracted from whole blood using PAXgene Blood RNA kits (QIAGEN Inc.) according to the manufacturer's protocol. The RNA was submitted to University of Minnesota Biomedical Genomics facility for quality controls, assessed by Agilent 2100Bioanalyzer (Agilent Technologies). One microgram of total RNA (with the integrity numbers >6.0) was used to prepare amplified and biotinylated antisense complementary RNA targets using the Illumina TotalPrep RNA amplification kit. Seven hundred nanograms of labeled complementary RNA were hybridized to human-HT-12v4 BeadChip arrays (Illumina Inc.), which contained 47 400 hybridization probes. The arrays were then washed, blocked, stained, and scanned on BeadStation500. The microarray data from this study has been deposited in the National Center for Biotechnology Information's Gene Expression Omnibus and are accessible through GEO Series ticket number no. 18800677 and will be available on January 10, 2019.

Microarray Signal Normalization and Statistical Data Analysis

Signal intensity values from the scans were generated using Illumina BeadStudio version 2 software. Raw microarray data were background subtracted, and $\log_2$ transformed (thus, 1.5-fold change cutoffs were chosen for downstream analysis). A stringent filter was implemented to select only those transcripts whose probe sets had at least 1 present detection above the background detection call, and missing intensity probes values were excluded. Datasets were normalized using the quintile interarray normalization method and exported into a Partek Genomic Suite version 6.6 (Partek Inc) for batch effect removal and statistical analysis. Batch effect was removed on random effects, such as date of microarray scan and the position of bead channels within microarray chips. Normalized gene expression values were considered for statistical analysis. Principal component analysis (PCA) visualized specimen-specific gene expression as PC correlations between groups (C-IRIS vs control) and subgroups (time points within each group and IRIS event). In the heat map visualizations of these data sets, the clustering was performed using both Euclidean and Pearson uncentered

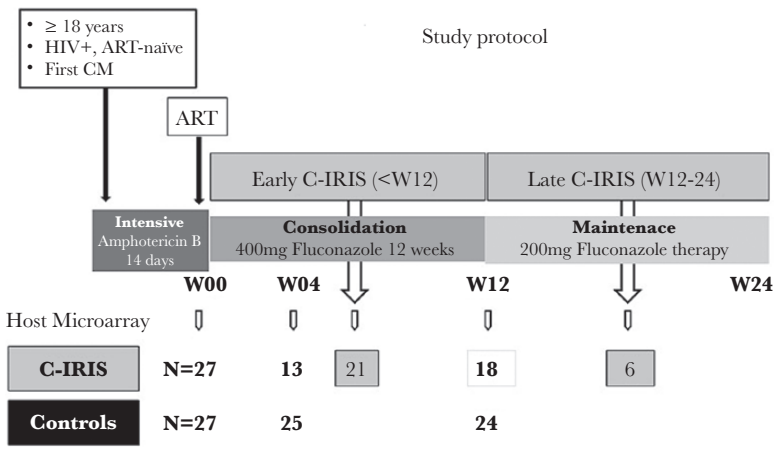

Figure 1. Study protocol, modified from Ref. [5]. Microarray blood collections were scheduled for W00 (pre-antiretroviral therapy [ART] initiation), W04, and W12 during the 24-week follow-up after ART. Additionally, blood samples were collected at time of the cryptococcosis-associated immune reconstitution inflammatory syndrome (C-IRIS) event—early (within 12 weeks) and late (between 12 and 24 weeks) of ART initiation.

distance metrics and average linkage-based algorithms to demonstrate how cases clustered based on RNA expression. Samples and differentially expressed probe sets were then ordered using hierarchical clustering such that groups and time points (within each group) could be distinguished according to similarities or differences in gene expression patterns. The list of differentially expressed genes was obtained from analysis of variance with restricted maximum likelihood (ANOVA-REML). Significantly changed probe intensities were filtered based on a minimum fold change threshold of 1.5 for up- or downregulation, in both groups at any time point. Values of *P* were corrected for multiple testing using the Benjamini-Hochberg false discovery rate.

Biomarkers Search

Predictor screening (based on Bootstrap Forest platform) was performed with standard parameters using JMP13 Pro (SAS Institute Inc.). Predictor screening allows simultaneous analysis of all variables for model validation within 2 groups (IRIS versus no IRIS), or within an analysis of 8 subgroups (control week 0, 4, 12 and IRIS week 0, 4, 12; early C-IRIS and late C-IRIS, respectively). For C-IRIS biomarker identification, the nonlinear iterative partial least squares (PLSs) algorithm with leave-one-out cross-validation method (available in JMP13 Pro) was used, which was carried out on 1700 transcripts. Variable Importance in the Projection (VIP) scores were extracted to reveal relations between predictors and outcome and plotted against coefficient of regression. Predictors and responses were scaled to have a mean of 0 and a standard deviation of 1 (by dividing each column by its standard deviation). To consider the transcript as a potential biomarker, the filters were set as such: the VIP score was >0.8 and the regression correlation coefficient was >0.2 in at least 1 of the studied subgroups. Model coefficients with their respective ranked VIP contributions are presented in Supplementary Table 3. The algorithm is available upon request.

Functional and Pathway Analysis

Ingenuity Pathways Analysis ([IPA] Ingenuity Systems Inc.) software was used to define biological networks, functional analyses of molecular interactions, and upstream regulators for the differentially expressed genes. The IPA workflow comprised core, functional, and canonical pathway analyses and was used as a reference data set. Both direct and indirect molecular relationships were included in the analysis settings, and the significance of relationships 1700 immune gene transcripts was indicated with z-score and Fisher's exact test *P* values <.05.

Quantitative Polymerase Chain Reaction Validation Assay

Quantitative real-time polymerase chain reaction (PCR) was performed in triplicate specimens for each transcript of interest. Relative concentrations were calculated against internally built standard curves. Complementary deoxyribonucleic acid was synthesized from 200 ng total cellular RNA using Strata Script TM III reverse transcriptase (Stratagene) using transcript-specific primers as described previously [12, 13]. The 600 ng of the pool of total RNA (per plate) was used to create for upper standard, which was titrated 1:3 to generate 4-point curve. The PCR amplifications were then performed using the SYBR Green PCR Kit (Bio-Rad Laboratories) according to manufacturer's instructions. Transcript-specific oligonucleotide primers were custom designed and synthesized by IDT Inc. The PCR amplification was done using an Mx3000 Stratagen thermocycler, and data were analyzed using MxPro version 4.01 software. Relative concentrations of each amplified transcript were normalized to the relative levels of the hypoxanthine phosphoribosyltransferase transcript synthesized from the same specimen. The plots were derived as follows: concentrations of control samples at baseline (W00) were set as **1**. The relative fold change expressions for control and C-IRIS groups were plotted longitudinally over 0, 4, 12-week time points; early/later C-IRIS events were correspondingly assigned to W03/W16.

RESULTS

Subjects enrolled into this study underwent approximately 2 weeks of induction antifungal therapy with amphotericin B and subsequently started ART. Figure 1 shows the time line of antifungal therapy, ART, C-IRIS events, and sample collection. Comparative demographic details of the original cohort of 130 participants and current substudy are found in Chang et al [5] and Akilimali et al [14] respectively, where the C-IRIS group and the control group without neurological deterioration showed no significant difference in age, gender, baseline HIV viral load, or serum cryptococcal antigen titers.

At the Time of Antiretroviral Therapy Initiation, Transcriptome Profiles Differed Between Cryptococcosis-Associated Immune Reconstitution Inflammatory Syndrome and Control Groups

We hypothesized that HIV-infected patients with CM who developed C-IRIS would show a transcriptomic signature of immune deactivation at the time of ART initiation. The ANOVA-REML analysis, using criteria described in the Methods, identified over 1000 differentially expressed transcripts between the C-IRIS and the control groups at the time of ART initiation. The C-IRIS samples exhibited decreased expression of transcripts associated with antiviral responses (Figure 2), specifically those that lead to downregulation of viral replication including interferon (IFN)-induced protein 44 (IFI44), and IFN-induced proteins with tetratricopeptide repeats (IFIT1-5). In addition, the DExH and DExD/H-Box helicases (DDX58, DHX58) and transcripts encoding enzymes that directly restrict or inhibit viral replication (eg, oligoadenylate synthases [OIS1–3]) were also downregulated in the C-IRIS group. This peripheral blood transcriptomic signature in the C-IRIS group reflected a paucity of expression of genes that play a significant role in cellular resistance to viral infections.

In contrast, the expression of transcripts encoding markers of activated granulocytes, tissue infiltration, and destruction

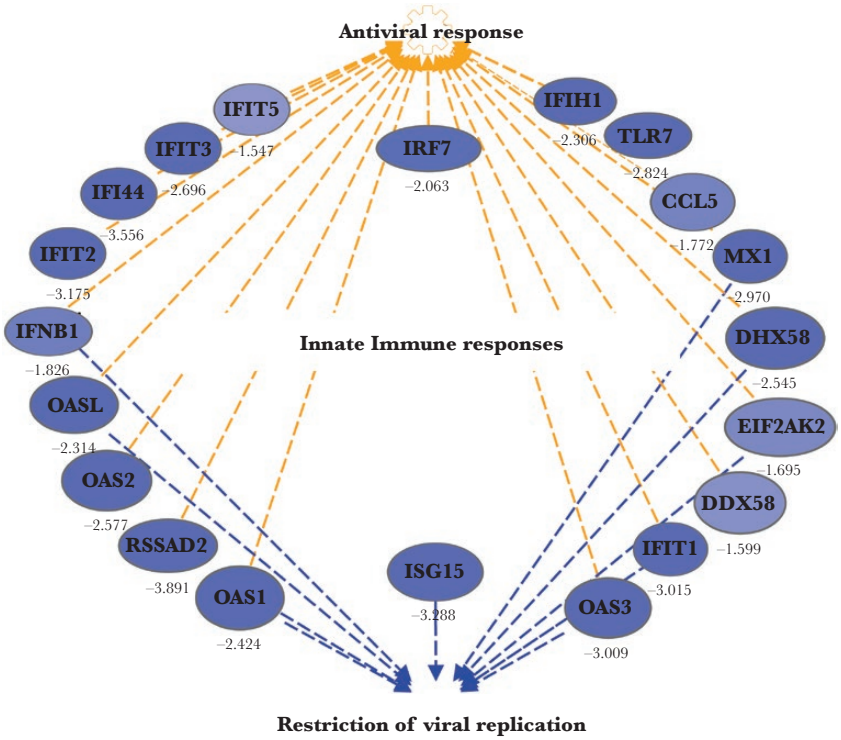

Figure 2. The low antiviral gene expressions at the time of antiretroviral therapy (ART) initiation in cryptococcosis-associated immune reconstitution inflammatory syndrome (C-IRIS) group. The C-IRIS group exhibited significantly lower expression of genes associated with innate immune responses: specifically, those that involve activation of antiviral defense (for example, interferon-inducible genes (IFI), and other, connected with orange lines), or genes encoding enzymes, that directly restrict or inhibit viral replication (for example, oligoadenylate synthase [OAS] or helicases [DHX]). Interferon-induced protein with tetratricopeptide repeats (IFIT) family genes are predominantly induced by type I and type III interferons and are regulated by the pattern recognition and the JAK-STAT signaling pathway. The OAS genes encode a synthase family that is induced by interferons and catalyze the 2′,5′-oligomers of adenosine to bind and activate RNase L. The IFIT and OAS families of genes are one of many interferon-stimulated genes that play a significant role in the inhibition of cellular protein synthesis in infected cells and is particularly important in cellular resistance to viral infections. Transcripts (nodes), colored in blue, were downregulated (>1.5-fold) with the intensity of blue reflecting the degree of downregulation. Fold change for these transcripts' expression is shown in Table 1. The orange line represents activation effect of the encoded protein. The blue line represents inactivation effect of the encoded protein. Transcripts were identified through functional analysis using Ingenuity Pathway Assistant (IPA) software.

were significantly higher expressed in subjects who subsequently developed C-IRIS (eg, matrix metallopeptidases or myeloperoxidases; see Table 1). Transcripts encoding C-type lectin domain family members (CLEC 5A, 1B, 4D) and the family of small antimicrobial cytotoxic peptides defensins (DEFA1, -3, -4, -5) also exhibited significantly increased expression in the C-IRIS group at baseline. Taken into account that defensins are more abundant in neutrophil granules, and CLECs play a role in MHCI Ca^{2+}-dependent pathogen recognition, this baseline transcriptomic signature suggests an activation of granulocyte-mediated inflammation, which may place patients at risk for the development of C-IRIS.

Antiretroviral Therapy-Associated Downregulation of Antiviral Proinflammatory Responses in the Control Group Is Seen Over 12 Weeks

Longitudinal data analysis in the control group identified 588 and 1412 differentially abundant transcripts at weeks 4 and 12, compared with W00 (pre-ART commencement). We detected longitudinal upregulation of transcripts such as interleukin (IL)7R, numerous cluster differentiation, and human leukocyte antigen molecules during 12 weeks on ART (see Supplementary Table 1). Such longitudinal increases in expression are a reflection of the effective immune recovery in lymphocyte populations and improvement in the antigen-presentation function in the control group. Functional analysis of downregulated transcripts indicated progressive decline of 2 predominant pathways: type I/II IFN-STAT signaling and nuclear factor (NF)-kB signaling (see Supplementary Figure 1).

Activation of these proinflammatory genes is often associated with cell death, thus the reduction of expression of these transcripts is beneficial for the effective immune reconstitution on ART [15]. On the contrary, the abundance of some IFN I/II-STAT and NF-kB signaling components had increased in the C-IRIS group at week 4 after ART, suggesting a switch to aberrant immune activation as presented below.

Altered Blood Transcriptomic Profiles in Subjects Who Developed Cryptococcosis-Associated Immune Reconstitution Inflammatory Syndrome

We hypothesized that HIV-infected patients with CM show a transcriptomic signature of aberrant immune activation in the blood during C-IRIS event. We performed

Table 1. Pre-ART Gene Expression in C-IRIS Versus Control Groups[a]

Gene Symbol, Biofunction	*P* Value, FDR	Fold Change
Antiviral Response		
IFI44L	2.2E-16	−4.5
IFI44	5.2E-16	−3.6
IFIT1	5.5E-11	−3.0
IFIT2	1.9E-21	−3.2
IFIT3	1.1E-13	−2.7
IFIT5	2.1E-08	−1.5
ISG15	3.0E-10	−3.3
OAS1	2.1E-17	−2.4
OAS2	2.7E-18	−2.6
OAS3	2.4E-17	−3.0
MX1	1.1E-16	−3.0
DDX58	1.6E-09	−1.6
TLR7	4.4E-27	−2.8
DHX58	1.8E-15	−2.5
Antimicrobial Response		
OLFM4	1.2E-28	8.6
CD177	2.8E-17	4.1
DEFA	6.7E-07	2.6
DEFA1B	4.8E-10	3.5
DEFA3	2.5E-09	3.1
DEFA4	9.4E-14	3.8
DEFA5	1.0E-22	1.6
DEFB106B	7.1E-18	1.5
CLEC5A	8.1E-21	3.3
CLEC4D	3.8E-11	2.0
CLEC1B	2.2E-10	2.2
CLECL1	1.6E-13	1.7
SIGLEC14	9.1E-03	2.1
Apoptosis		
MMP9	9.9E-10	3.0
MMP8	7.3E-28	6.9
MPO	1.7E-20	2.9
C1QTNF5	1.6E-25	2.4
ARG1	1.7E-17	3.7
LCN2	1.9E-24	5.8

Abbreviations: ART, antiretroviral therapy; C-IRIS, cryptococcosis-associated immune reconstitution inflammatory syndrome; FDR, false discovery rate; GO, Gene Ontology.

[a]Transcript symbol, abbreviated transcript name. Positive values, upregulated; negative values, downregulated between 2 baselines (week 00). Biofunction as defined in the GO database.

PCA to visualize the differences in gene expression levels in the entire dataset. Figure 3A depicts distinct separation between C-IRIS and control samples (PCA1). The PCA2 segregated samples collected (1) at scheduled visits (week 0, 4, and 12) longitudinally within C-IRIS and control groups and (2) at time of C-IRIS event. Moreover, PCA3 clustered together samples from IRIS events that occurred within first 12 weeks on ART (early C-IRIS) and separately from C-IRIS events that occurred after 12 weeks (late C-IRIS). This segregation of transcriptomic profiles suggests that although early and late C-IRIS events have seemingly similar clinical manifestations, they differ significantly in transcriptomic signature.

Early Cryptococcosis-Associated Immune Reconstitution Inflammatory Syndrome (C-IRIS) Events Were Characterized by Upregulation of Innate Immune Response Genes, Whereas Late C-IRIS Events Showed Deregulation of Genes in Adaptive Immune Response Pathways

Using Partek Genomics Suite software, we obtained a similarity matrix based on the hierarchical clustering (as described in Methods) to identify differences in transcript expression at early versus late C-IRIS events (Figure 3B and Supplementary Figure 3). The ANOVA-REML analysis identified 539 and 1143 transcripts that were differentially expressed at the time of early or late C-IRIS events, respectively, compared with W00. Early C-IRIS events were characterized by upregulation of numerous transcripts involved in innate immune responses: for example, upregulation of transcripts involved in inflammasome pathways, such as, absent in melanoma AIM2, caspases, IL1B, and NLR family domain containing transcripts (Figure 4). Inflammasome components are part of the larger molecular network of pattern-recognition receptors (PRRs), including Toll-like receptors (TLRs) and cytosolic surveillance pathway molecules, many of which were also upregulated (Supplementary Figure 2). The PRRs recognize diverse pathogen-associated molecular pattern (PAMPs) molecules found in variety of microorganisms, including *Cryptococcus* species [16, 17].

Late C-IRIS also exhibited the upregulation of transcripts involved in the inflammasome signaling pathway, such as CASP5 and AIM2. However, late C-IRIS events were primarily characterized by upregulation of CD2, CD3, CD8, CD302 (expressed on T and B cells), and CD160, killer cell lectin-like receptors (expressed on NK cells), and also IFN gamma (IFNG), granzymes, and other mediators of inflammation, compared with W00. In addition, we compared gene expression at the 12-week time point in the C-IRIS group with corresponding gene expression samples at late C-IRIS events, aiming to identify gene expression pattern that precedes late C-IRIS. At the time-point preceding the onset of late C-IRIS (W12) compared to at the time of late C-IRIS, we found increased expression of transcripts encoding for CCL-, CCR-, CXCR-type chemokines and chemokine receptors, and adhesion molecules such as integrins, selectins and claudins. The fold change expression values for these molecules can be found in Supplementary Table 2. These findings suggest that systemic upregulation of transcripts involved in inflammatory immune cell migration occurs in peripheral blood before the development of late C-IRIS.

We analyzed the enrichment of canonical pathways using IPA software, for early and late C-IRIS subgroups. The top 5 canonical pathways with altered expression at the time of early C-IRIS (Figure 5A) represent the activation of recognition of bacteria and viruses through cytosolic PRRs. All 5 pathways encode components of innate immunity and could be considered as drivers of early C-IRIS. The late C-IRIS is driven by molecular pathways that included transcripts involved in T- and B-cell signaling, NK cell signaling, and apoptosis (Figure 5B). In addition, we used IPA causal network analysis to detect upstream

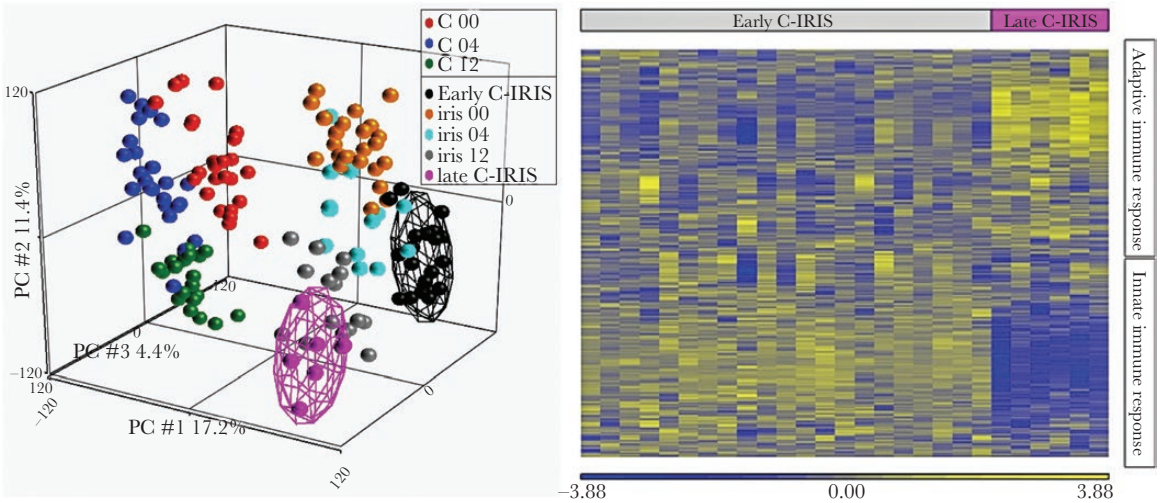

Figure 3. Identification of cryptococcosis-associated immune reconstitution inflammatory syndrome (C-IRIS) features through unsupervised learning algorithms. (A) Principal component (PC) analysis showed distinct patterns in ribonucleic acid (RNA) expression between C-IRIS patients and controls. Using all 34 668 expressed probe identifiers and 162 individual arrays, 3 PCs accounted for 33% total variance in gene expression, (PC#1 17.2%, PC#2 11.4%, PC#3 4.4%, respectively). Samples were color coded by study subgroups (see legend). Ellipsoids are drawn around samples that represent 2 standard deviations, for early (black) and late (pink) C-IRIS events. (B) Hierarchical clustering analysis of 1700 probe IDs representing immune genes that were differentially expressed between early and late C-IRIS events. Hierarchical clustering is built based on normalized log-transformed gene expression values. Heatmap coloring is based on expression levels: yellow, high level of expression; blue, low level of expression. Both rows and columns are hierarchically clustered according to the Pearson's average linkage dissimilarity method in Partek Genomics Suite (GS). Top gray bar represents early C-IRIS, and pink bar represents late C-IRIS (individual cases).

regulatory molecules, affecting gene expression during C-IRIS events. This analysis predicted that PAMPs molecules were upstream regulators of early C-IRIS (shown in Supplementary Figure 2), consistent with our finding that transcripts encoding TLR/inflammasome pathways were upregulated. In contrast, IFNG, IL2, and IL21 were predicted to be upstream regulators of late C-IRIS gene expression. Thus, early and late C-IRIS events appeared to be due to overexuberant inflammatory responses that are driven by different signaling cascades for early versus late C-IRIS events.

Biomarkers of Early and Late Cryptococcosis-Associated Immune Reconstitution Inflammatory Syndrome

The next step was to identify transcripts that may be predictive biomarkers of C-IRIS events, utilizing 2 independent computational algorithms available in JMP Pro13: the predictor screening (based on random bootstrap forest algorithm [RBSF]) and PLS probability modeling. The RBSF algorithm was performed on all 34 668 probe IDs expressed on microarrays. The top 200 high-rank importance predictors whose expression distinguished C-IRIS from other subgroups is listed in Supplementary Table 3.2. Among them was the inhibitor of differentiation (ID4), bone barrow stromal antigen (BST1), and IL32, suggesting a strong contribution of abnormal cellular differentiation and proliferation processes into C-IRIS onset. One interesting transcript, BEX1 (brain-expressed X-linked protein-1), that was steadily upregulated in C-IRIS group at all time points could represent a predictive peripheral blood biomarker of neuroinflammation. The majority of the identified biomarkers remain annotated, highlighting that we were only beginning to unravel the complex nature of immune reconstitution. Aiming to identify immune biomarkers of C-IRIS events, we exported from IPA software all annotated immune genes that are significantly changed, at any time point of observation post-ART.

This export generated 1700 transcripts, which were analyzed with PLS and RBSF algorithms. The PLS analysis was performed on the two groups of samples: early C-IRIS, late C-IRIS, and no C-IRIS and on all subgroups, including all time points within each group. A quantitative estimation of the discriminatory power of each predictor in PLS is provided by means of VIP scores (listed in Supplementary Table 3.3, 3.4, 3.5). Subgroup analysis revealed that most of the top ranked biomarkers were specific for either early or late C-IRIS and anticorrelate with each other: for example, differential expression of transcripts encoding of CCL8, CASP12, DDX58, and tumor necrosis factor (TNF) positively correlated with early C-IRIS events (VIP > 0.8, R > 0.2) but negatively correlated with late C-IRIS (VIP > 0.8, R > −0.2). The differential expression of transcripts encoding C-type lectins (CLECs) and sialic acid binding immunoglobulin-like lectins (SIGLECs) positively predicted early C- IRIS but not with late C-IRIS. A particularly high association of coexpression of IFNG, complement pathway component C1QC, and IL27 were uniquely observed in late C-IRIS. It is interesting to note that elevated expression of transcripts that reflect neuronal apoptotic processes or neurological deterioration, such as galectins, ephrin receptors, and kallikreins, were significantly upregulated in both early and late C-IRIS events ($P < .01$). Low baseline expression of IFN-response genes (TLR2 and -7,

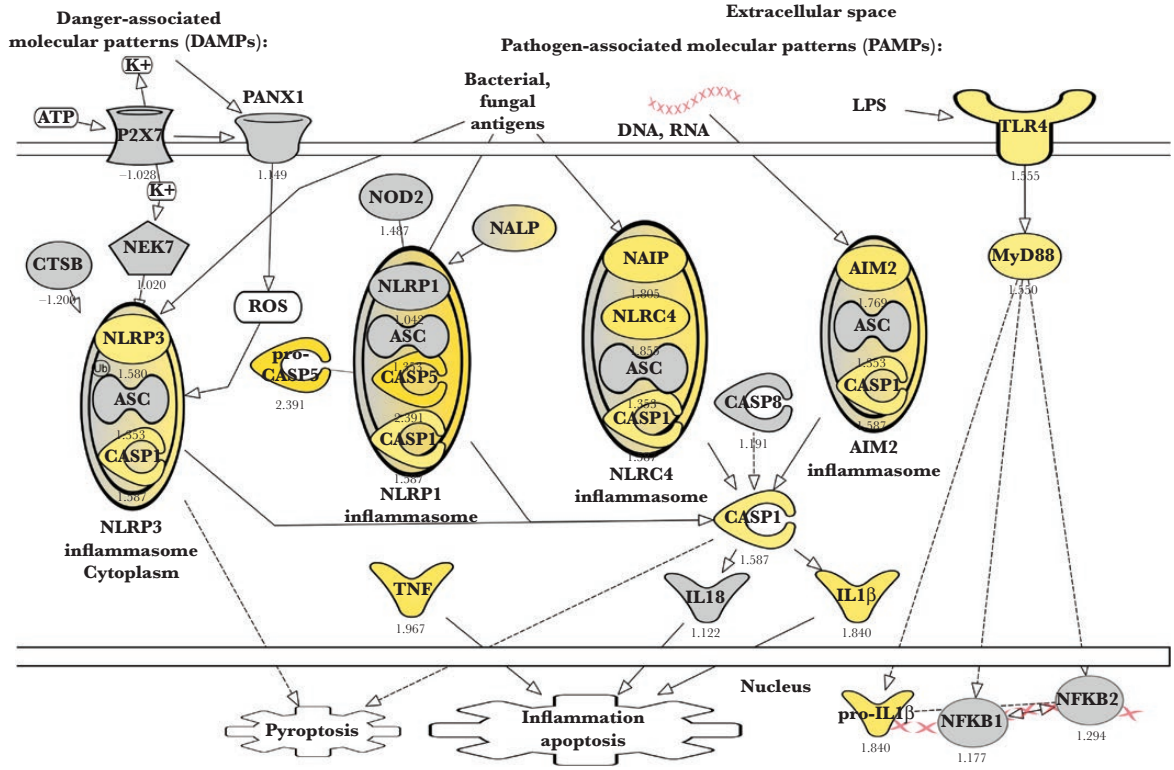

Figure 4. Transcriptomic signature of early cryptococcosis-associated immune reconstitution inflammatory syndrome (C-IRIS) events (<week 12 of antiretroviral therapy [ART] initiation). The inflammasome pathway is shown. Transcripts, colored in yellow, are upregulated >1.5-fold in early C-IRIS samples, with the intensity of yellow reflecting the degree of upregulation ($P < .05$). Fold changes of upregulation (early C-IRIS versus W00 in IRIS group samples) are shown below the nodes. Nodes in gray are significantly differently expressed ($P < .05$), with less than 1.5-fold change expression. The intensity of color reflects the degree of changes.

DEFA3, and CD69) predicted subsequent early and late C-IRIS, after ART commencement. The correlation coefficients for least square mean and a corresponding statistical VIP (values ranking descriptors) for 13 transcripts that identified by both algorithms can be found in Supplementary Table 3.1. All of these transcripts represent novel biomarkers of C-IRIS.

Biomarker Validation

We used real-time quantitative PCR to validate the differential expression of messenger RNA (mRNA) for 15 selected genes as described in Methods, and the results are shown in Supplementary Figure 4A–D. Supplementary Figure 4A depicts the expression profiles for biomarkers of both C-IRIS events, which were persistently elevated in both C-IRIS subgroups over 12 weeks of observation: AIM2, BEX1, C1QB (>1.5-fold in expression). The CASP5, DDX58, and TNF mRNA levels were upregulated >2-fold in early C-IRIS patients and subsequently downregulated by week 12, although not to the level of control mRNAs (Supplementary Figure 4B). Compared with the baseline, the late C-IRIS patients exhibited significantly higher levels of IFNG, IL27, and KLRB1 transcripts after 12 weeks of observation, but they had very low expression of these transcripts at baseline, compared with control samples (see Supplementary Figure 4C). We validated several biomarkers that constitutes favorable immune recovery: the antiviral defense transcripts were upregulated at baseline in the control group (IFI44, IRF7, MX1) and had distinct downregulation profiles over 12 weeks of observation, compared with C-IRIS group (see Supplementary Figure 4D). At baseline, the levels of antimicrobial defense mRNAs (DEFA3, CLEC5A, CD69) were higher in the C-IRIS group compared with the control group (Supplementary Figure 4E). The levels of these transcripts subsequently decreased even more in the control group, but not in the early C-IRIS group. Overall, the expression profiles for these transcripts were similar for the real-time quantitative PCR results and the microarray results.

DISCUSSION

Cryptococcosis-associated immune reconstitution inflammatory syndrome has emerged as an important complication of ART in HIV-CM coinfection. Utilizing longitudinal data analysis of samples from a well characterized prospective cohort of HIV-CM-coinfected patients initiating ART, who experienced C-IRIS compared with $CD4^+$ T cell-matched controls [5], we showed that C-IRIS subjects exhibited significantly lower expression of transcripts encoding antiviral defense proteins and upregulation of antimicrobial defense genes before ART commencement. Poor cellular antiviral and inflammatory responses in cerebrospinal fluid (CSF) have been suggested to

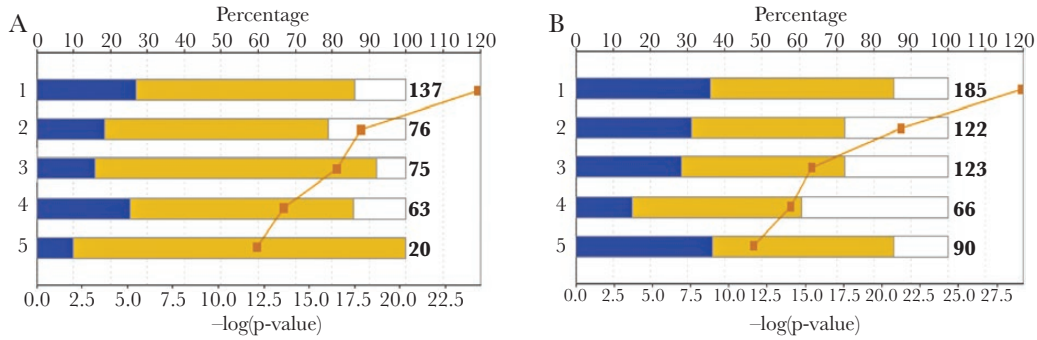

Figure 5. Top 5 canonical pathways that were overrepresented in up- or downregulated transcripts in (A) early and (B) late cryptococcosis-associated immune reconstitution inflammatory syndrome (C-IRIS) subgroups. The top 5 canonical pathways (left axis) are displayed as stacked bar charts with percentage (top axis) of processes enriched by upregulated genes (yellow), by downregulated genes (blue), and those without a detectable change (white). The orange line graph represents the negative log-transformed *P* values (–log(*P*-value)) calculated by Fisher's exact test (bottom axis) for the association between Ingenuity Pathway Assistant (IPA)-annotated genes within the pathway (assumed 100%) and the number of genes found in the uploaded dataset (numbers on the top of the bar). (A) The top 5 canonical pathways with altered expression at the time of early C-IRIS: (1) role of pattern recognition of bacteria and viruses (137); (2) activation of interferon regulatory factors (IRF) by cytosolic pattern recognition receptors (63); (3) the triggering receptor expressed on myeloid cells 1 (TREM1) signaling (75); (4) inflammasome (20); (5) Toll-like receptor signaling (76). There was a minimal overlap in the transcripts between pathways, varying between 0 and 5 molecules. (B) The top 5 canonical pathways with altered expression at the time of late C-IRIS: (1) Th1 and Th2 activation (185); (2) natural killer cell signaling (122); (3) inducible costimulatory (iCOS)-iCOS ligand (iCOSL) signaling (123); (4) calcium-induced T lymphocyte apoptosis (66); (5) altered T and B signaling in inflammation (90). There was a minor overlap in the transcripts between pathways, varying between 3 and 11 molecules.

be associated with poor CM outcomes and predispose patients to IRIS [5, 6, 18, 19]. Low CSF levels of IFNG have been previously shown to be associated with poorer CSF clearance of cryptococci, and, in 2 studies, adjunctive IFNG treatment has been shown to improve rate of CSF clearance [20, 21]. We have previously shown that IFNG secretion in whole blood stimulated with cryptococcal mannoprotein is reduced in C-IRIS before ART initiation [22]. In this study, the predictor screening algorithms identified the low expression of the components of antiviral defense pathway, such as IFN-inducible genes, as predictive biomarkers of subsequent C-IRIS. Thus, the paucity of antiviral gene expressions in peripheral blood at the time of ART initiation could have predictive value for identifying those at risk for C-IRIS. Patients who exhibit such signatures also display activation of granulocyte-dependent proinflammatory responses (through upregulation of CLECs and DEFAs) and may require longer antifungal therapy before initiation of ART to achieve clearance and reduce risk of C-IRIS [23]. We have previously shown that HIV-CM-coinfected patients who were able to achieve cryptococcal culture negativity in the CSF before ART initiation compared with those with residual cryptococcal positive cultures were associated with reduced neurological deterioration, C-IRIS, and cryptococcal relapse [5]. Others have shown that patients who initiate ART early compared with late in HIV-CM coinfection have increased mortality [24, 25] and increased C-IRIS incidence [26]. Thus, an initial effective immune response, characterized by adequate production of IFNs and IFN-response genes, may lead to better antigen clearance and improved outcomes.

The course of immune recovery on ART in our control group is similar to that previously demonstrated in advanced stage HIV-infected patients without opportunistic infections, where maintenance of innate host defenses in an activated state through the IFN I/II-STAT pathway was seen prior to ART initiation and subsequently declined on ART [15]. While this and our previous study showed that IFN I/II pathway were down-regulated early in the controls, the IFNG pathway remained inert in the C-IRIS group even post-ART [15]. Our results suggest that the differences in longitudinal transcriptomic profiles of those with or without C-IRIS gives insight into what constitutes an effective response that leads to immune recovery on ART, as opposed to a pathological response that leads to C-IRIS.

Moreover, the C-IRIS group exhibited abnormal longitudinal proinflammatory changes in gene expression profiles that were evident in the blood weeks after ART initiation and transition onto fluconazole maintenance therapy, as discussed below. There was a significant modification in gene expression signatures and differences in identified biomarkers seen in late C-IRIS events versus early C-IRIS, suggesting that early and late C-IRIS have distinct molecular phenotypes. The AIM2, C1QB, and BEX1 were identified as common biomarkers for both early and late C-IRIS events, and thus they warrant future investigation. Early C-IRIS was associated with upregulation in innate responses, and late C-IRIS had more pronounced signature of adaptive immune activation. Unlike in immunocompetent patients [27], in immunocompromised patients the innate immune system is the primary branch that elicits immune response to combat opportunistic infections. Overactivation of it through PRR signaling

sets up a cycle of local and systemic inflammation [28]. In our study, TLR and inflammasome components (including AIM2, CASP5, and NLR families), identified as biomarkers of early C-IRIS events; these may represent a response toward ongoing viral replication and cryptococcal antigens. Recent data suggest that the inflammasome pathway drives $CD4^+$ T-cell depletion in HIV-1 infection [29] and delays immune reconstitution. Thus, inflammasome activation may contribute to the neurological deterioration symptoms seen in C-IRIS patients, which has been also proposed for tuberculosis meningitis IRIS (TBM-IRIS) [30–33], and represent a peripheral blood biomarker of brain inflammation for both CM and TBM-IRIS. Other identified biomarker transcripts that reflected innate immune responses specifically toward cryptococcal antigen (eg, CLECs, SIGLECs, dectins) should also be further studied in depth to understand the pathogenesis of immune reconstitution in C-IRIS patients.

The findings seen in late C-IRIS such as activation of components of complement and the inflammasome, along with IFNG, IL27, KLRB1, and other transcripts expressed in T, B, and NK cells, suggest an impaired restoration of adaptive immunity. Poor recovery of adaptive immunity and impaired communication between innate and adaptive immune branches due to lack of negative regulatory feedback responses leads to an inability to resolve inflammation [34]. The onset of late C-IRIS is preceded by excessive expression of chemokines and integrins in peripheral blood, and thus may be predicted through monitoring the aberrant kinetics of immune reconstitution in patients at risk. In this study, we identified a number of biomarker transcripts that encode intracellular molecules expressed in various circulating immune cells. We hypothesize that transcripts (AIM2, C1QB, and BEX1) which were identified by 2 predictor algorithms may compose a bundle biomarker signature of neuroinflammation during the complex, antigen-driven process of immune reconstitution. One limitation of this study is that we did not systematically look for other opportunistic infections that might be present in these patients (such as tuberculosis, toxoplasmosis, cytomegalovirus, etc), because these unknown factors may have skewed our results. Further in-depth study and interpretation of the biological processes associated with the biomarkers identified through statistical modeling in our study will enhance the robustness of our findings [35].

CONCLUSIONS

In conclusion, the information presented in this report provides insight into the molecular drivers of C-IRIS pathogenesis and can be applied in the future to developing diagnostic tests that guide targeted immunomodulatory treatments.

Supplementary Data

Supplementary materials are available at *Open Forum Infectious Diseases* online. Consisting of data provided by the authors to benefit the reader, the posted materials are not copyedited and are the sole responsibility of the authors, so questions or comments should be addressed to the corresponding author.

Acknowledgments

We acknowledge the patients and research investigators of the parent cryptococcosis-associated immune reconstitution inflammatory syndrome (C-IRIS) study, including the clinical and laboratory staff at King Edward VIII hospital and HIV Pathogenesis Programme, Durban, South Africa. Our special thanks to Professor Thumbi Ndung'u for providing the facilities for samples storage. We acknowledge the University of Minnesota Supercomputing Institute for providing the access to Ingenuity Pathway Assistant and University Biomedical Genomics facility for hybridizing and scanning microarrays. We thank Tawa Alabi, Ashley Johnson, and Calandra Sagarsky for experimental assistance.

Author contributions. I. V.-S. and C. C. C contributed equally to this work; C. C. C. directed the clinical study; I. V.-S. directed the genomics study and data analysis; S. S. performed experiments; I. V.-S., C. C. C., P. R. B., and M. A. F. wrote and edited the manuscript.

Financial support. This work is funded by a University of Minnesota departmental start-up fund (to I. V.-S.) and National Institutes of Health grant AI072068 (to P. R. B.). C. C. C. is supported by an Australian National Health and Medical Research Council Early Career Fellowship (1092160).

Potential conflicts of interest. All authors: No reported conflicts of interest. All authors have submitted the ICMJE Form for Disclosure of Potential Conflicts of Interest.

References

1. Rajasingham R, Rhein J, Klammer K, et al. Epidemiology of meningitis in an HIV-infected Ugandan cohort. Am J Trop Med Hyg **2015**; 92:274–9.
2. Rajasingham R, Smith RM, Park BJ, et al. Global burden of disease of HIV-associated cryptococcal meningitis: an updated analysis. Lancet Infect Dis **2017**; 17:873–81.
3. Haddow LJ, Colebunders R, Meintjes G, et al. Cryptococcal immune reconstitution inflammatory syndrome in HIV-1-infected individuals: proposed clinical case definitions. Lancet Infect Dis **2010**; 10:791–802.
4. Müller M, Wandel S, Colebunders R, et al. Immune reconstitution inflammatory syndrome in patients starting antiretroviral therapy for HIV infection: a systematic review and meta-analysis. Lancet Infect Dis **2010**; 10:251–61.
5. Chang CC, Dorasamy AA, Gosnell BI, et al. Clinical and mycological predictors of cryptococcosis-associated immune reconstitution inflammatory syndrome. AIDS **2013**; 27:2089–99.
6. Boulware DR, Bonham SC, Meya DB, et al. Paucity of initial cerebrospinal fluid inflammation in cryptococcal meningitis is associated with subsequent immune reconstitution inflammatory syndrome. J Infect Dis **2010**; 202:962–70.
7. Meya DB, Manabe YC, Boulware DR, Janoff EN. The immunopathogenesis of cryptococcal immune reconstitution inflammatory syndrome: understanding a conundrum. Curr Opin Infect Dis **2016**; 29:10–22.
8. Nelson AM, Manabe YC, Lucas SB. Immune reconstitution inflammatory syndrome (IRIS): what pathologists should know. Semin Diagn Pathol **2017**; 34:340–51.
9. Williamson PR, Jarvis JN, Panackal AA, et al. *Cryptococcal meningitis*: epidemiology, immunology, diagnosis and therapy. Nat Rev Neurol **2017**; 13:13–24.
10. Boulware DR, Meya DB, Bergemann TL, et al. Clinical features and serum biomarkers in HIV immune reconstitution inflammatory syndrome after cryptococcal meningitis: a prospective cohort study. PLoS Med **2010**; 7:e1000384.
11. Jarvis JN, Casazza JP, Stone HH, et al. The phenotype of the Cryptococcus-specific CD4+ memory T-cell response is associated with disease severity and outcome in HIV-associated cryptococcal meningitis. J Infect Dis **2013**; 207:1817–28.
12. Vlasova IA, McNabb J, Raghavan A, et al. Coordinate stabilization of growth-regulatory transcripts in T cell malignancies. Genomics **2005**; 86:159–71.
13. Vlasova IA, Tahoe NM, Fan D, et al. Conserved GU-rich elements mediate mRNA decay by binding to CUG-binding protein 1. Mol Cell **2008**; 29:263–70.
14. Akilimali NA, Chang CC, Muema DM, et al. Plasma but not cerebrospinal fluid interleukin 7 and interleukin 5 levels pre-antiretroviral therapy commencement predict Cryptococcosis-associated immune reconstitution inflammatory syndrome. Clin Infect Dis **2017**; 65:1551–9.
15. Boulware DR, Meya DB, Bergemann TL, et al. Antiretroviral therapy down-regulates innate antiviral response genes in patients with AIDS in sub-saharan Africa. J Acquir Immune Defic Syndr **2010**; 55:428–38.
16. Ellerbroek PM, Walenkamp AM, Hoepelman AI, Coenjaerts FE. Effects of the capsular polysaccharides of *Cryptococcus neoformans* on phagocyte migration and inflammatory mediators. Curr Med Chem **2004**; 11:253–66.
17. Hole C, Wormley FL Jr. Innate host defenses against *Cryptococcus neoformans*. J Microbiol **2016**; 54:202–11.

18. Boulware DR, von Hohenberg M, Rolfes MA, et al. Human immune response varies by the degree of relative cryptococcal antigen shedding. Open Forum Infect Dis **2016**; 3:ofv194.
19. Scriven JE, Graham LM, Schutz C, et al. A glucuronoxylomannan-associated immune signature, characterized by monocyte deactivation and an increased interleukin 10 level, is a predictor of death in cryptococcal meningitis. J Infect Dis **2016**; 213:1725–34.
20. Pappas PG, Bustamante B, Ticona E, et al. Recombinant interferon-gamma 1b as adjunctive therapy for AIDS-related acute cryptococcal meningitis. J Infect Dis **2004**; 189:2185–91.
21. Jarvis JN, Meintjes G, Rebe K, et al. Adjunctive interferon-γ immunotherapy for the treatment of HIV-associated cryptococcal meningitis: a randomized controlled trial. AIDS **2012**; 26:1105–13.
22. Chang CC, Lim A, Omarjee S, et al. Cryptococcosis-IRIS is associated with lower cryptococcus-specific IFN-γ responses before antiretroviral therapy but not higher T-cell responses during therapy. J Infect Dis **2013**; 208:898–906.
23. Dyal J, Akampurira A, Rhein J, et al. Reproducibility of CSF quantitative culture methods for estimating rate of clearance in cryptococcal meningitis. Med Mycol **2016**; 54:361–9.
24. Makadzange AT, Ndhlovu CE, Takarinda K, et al. Early versus delayed initiation of antiretroviral therapy for concurrent HIV infection and cryptococcal meningitis in sub-saharan Africa. Clin Infect Dis **2010**; 50:1532–8.
25. Boulware DR, Meya DB, Muzoora C, et al. Timing of antiretroviral therapy after diagnosis of cryptococcal meningitis. N Engl J Med **2014**; 370:2487–98.
26. Bisson GP, Nthobatsong R, Thakur R, et al. The use of HAART is associated with decreased risk of death during initial treatment of cryptococcal meningitis in adults in Botswana. J Acquir Immune Defic Syndr **2008**; 49:227–9.
27. Panackal AA, Wuest SC, Lin YC, et al. Paradoxical immune responses in non-HIV cryptococcal meningitis. PLoS Pathog **2015**; 11:e1004884.
28. Lai RP, Meintjes G, Wilkinson KA, et al. HIV-tuberculosis-associated immune reconstitution inflammatory syndrome is characterized by Toll-like receptor and inflammasome signalling. Nat Commun **2015**; 6:8451.
29. Doitsh G, Galloway NL, Geng X, et al. Cell death by pyroptosis drives CD4 T-cell depletion in HIV-1 infection. Nature **2014**; 505:509–14.
30. Marais S, Lai RP, Wilkinson KA, et al. Inflammasome activation underlies central nervous system deterioration in HIV-associated tuberculosis. J Infect Dis **2016**; 215:677–86.
31. Oliver BG, Elliott JH, Price P, et al. Mediators of innate and adaptive immune responses differentially affect immune restoration disease associated with *Mycobacterium tuberculosis* in HIV patients beginning antiretroviral therapy. J Infect Dis **2010**; 202:1728–37.
32. Tan HY, Yong YK, Andrade BB, et al. Plasma interleukin-18 levels are a biomarker of innate immune responses that predict and characterize tuberculosis-associated immune reconstitution inflammatory syndrome. AIDS **2015**; 29:421–31.
33. Tan HY, Yong YK, Shankar EM, et al. Aberrant inflammasome activation characterizes tuberculosis-associated immune reconstitution inflammatory syndrome. J Immunol **2016**; 196:4052–63.
34. Antonelli LR, Mahnke Y, Hodge JN, et al. Elevated frequencies of highly activated CD4+ T cells in HIV+ patients developing immune reconstitution inflammatory syndrome. Blood **2010**; 116:3818–27.
35. Selvan LD, Sreenivasamurthy SK, Kumar S, et al. Characterization of host response to *Cryptococcus neoformans* through quantitative proteomic analysis of cryptococcal meningitis co-infected with HIV. Mol Biosyst **2015**; 11:2529–40.